Eur Radiol (2016) 26:4162–4172
DOI 10.1007/s00330-016-4276-8

HEAD AND NECK

Dynamic contrast-enhanced MRI, diffusion-weighted MRI and ^{18}F-FDG PET/CT for the prediction of survival in oropharyngeal or hypopharyngeal squamous cell carcinoma treated with chemoradiation

Shu-Hang Ng[1,2,3] · Chun-Ta Liao[4] · Chien-Yu Lin[5] · Sheng-Chieh Chan[1,6] · Yu-Chun Lin[2,3] · Tzu-Chen Yen[1,6] · Joseph Tung-Chieh Chang[5] · Sheung-Fat Ko[2] · Kang-Hsing Fan[5] · Hung-Ming Wang[7] · Lan-Yan Yang[8] · Jiun-Jie Wang[3,9,10,11]

Received: 7 August 2015 / Revised: 3 February 2016 / Accepted: 8 February 2016 / Published online: 24 February 2016

Abstract

Objectives We prospectively investigated the roles of pretreatment dynamic contrast-enhanced MR imaging (DCE-MRI), diffusion-weighted MR imaging (DWI) and ^{18}F-fluorodeoxyglucose-positron emission tomography (^{18}F-FDG PET)/CT for predicting survival of oropharyngeal or hypopharyngeal squamous cell carcinoma (OHSCC) patients treated with chemoradiation.

Methods Patients with histologically proven OHSCC and neck nodal metastases scheduled for chemoradiation were eligible. Clinical variables as well as DCE-MRI-, DWI- and ^{18}F-FDG PET/CT-derived parameters of the primary tumours and metastatic neck nodes were analysed in relation to 3-year progression-free survival (PFS) and overall survival (OS) rates.

Results Eighty-six patients were available for analysis. Multivariate analysis identified the efflux rate constant (K_{ep})-tumour < 3.79 min^{-1} ($P = 0.001$), relative volume of extracellular extravascular space (V_e)-node < 0.23 ($P = 0.004$) and SUV_{max}-tumour > 19.44 ($P = 0.025$) as independent risk factors for both PFS and OS. A scoring system based upon the sum of each of the three imaging parameters allowed stratification of our patients into three groups (patients with 0/1 factor, patients with 2 factors and patients with 3 factors, respectively) with distinct PFS (3-year rates = 72 %, 38 % and 0 %, $P < 0.0001$) and OS (3-year rates = 81 %, 46 % and 20 %, $P < 0.0001$).

Conclusions K_{ep}-tumour, V_e-node and SUV_{max}-tumour were independent prognosticators for OHSCC treated with chemoradiation. Their combination helped survival stratification.

Shu-Hang Ng and Chun-Ta Liao contributed equally to this work.

✉ Jiun-Jie Wang
jwang@mail.cgu.edu.tw

[1] Molecular Imaging Center, Chang Gung Memorial Hospital, Chang Gung University, Kueishan, Taoyuan, Taiwan

[2] Department of Diagnostic Radiology, Chang Gung Memorial Hospital, Chang Gung University, Kueishan, Taoyuan, Taiwan

[3] Department of Medical Imaging and Radiological Sciences, Chang Gung Memorial Hospital, Chang Gung University, 259 Wen Hua 1st Road, Kueishan, Taoyuan 333, Taiwan

[4] Department of Otorhinolaryngology, Head and Neck Surgery, Chang Gung Memorial Hospital, Chang Gung University, Kueishan, Taoyuan, Taiwan

[5] Department of Radiation Oncology, Chang Gung Memorial Hospital, Chang Gung University, Kueishan, Taoyuan, Taiwan

[6] Department of Nuclear Medicine, Chang Gung Memorial Hospital, Chang Gung University, Kueishan, Taoyuan, Taiwan

[7] Department of Medical Oncology, Chang Gung Memorial Hospital, Chang Gung University, Kueishan, Taoyuan, Taiwan

[8] Biostatistics and Informatics Unit, Chang Gung Memorial Hospital, Chang Gung University, Kueishan, Taoyuan, Taiwan

[9] Neuroscience Research Center, Chang Gung Memorial Hospital, Taoyuan, Taiwan

[10] Department of Diagnostic Radiology, Chang Gung Memorial Hospital, Keelung, Taiwan

[11] Medical Imaging Research Center, Institute for Radiological Research, Chang Gung University / Chang Gung Memorial Hospital, Linkou, Taoyuan, Taiwan

Key Points

- *K_{ep}-tumour, V_e-node and SUV_{max}-tumour are independent predictors of survival rates.*
- *The combination of these three prognosticators may help stratification of survival.*
- *MRI and FDG-PET/CT play complementary roles in prognostication of head and neck cancer.*

Keywords Oropharyngeal cancer · Hypopharyngeal cancer · Dynamic contrast-enhanced MRI · Diffusion-weighted imaging · Chemoradiation · Survival

Abbreviations

ADC	apparent diffusion coefficient
DCE-MRI	dynamic contrast-enhanced magnetic resonance imaging
DWI	diffusion-weighted imaging
^{18}F-FDG PET/CT	^{18}F-fluorodeoxyglucose-positron emission tomography/computed tomography
HNSCC	head and neck squamous cell carcinoma
K_{ep}	efflux rate constant
K^{trans}	volume transfer rate constant
MTV	metabolic tumour volume
OHSCC	oropharyngeal or hypopharyngeal squamous cell carcinoma
OS	overall survival
PFS	progression-free survival
SUV_{max}	maximum standardized uptake value
TLG	total lesion glycolysis
V_e	relative volume of extracellular extravascular space
V_p	relative vascular plasma volume

Introduction

Oropharyngeal and hypopharyngeal squamous cell carcinomas (OHSCC) are head and neck cancers that arise from adjacent anatomic areas. These cancers share both similar lymphatic drainage and treatment approaches. Most patients with OHSCC have advanced cancer staging at presentation with aggressive local invasion or malignant cervical adenopathy. Although chemoradiation is currently considered as the mainstay of organ-sparing therapy for OHSCC [1], treatment outcomes remain unsatisfactory especially in the presence of advanced disease. In a series of 65 stage III/IV OHSCC patients undergoing chemoradiation, Wang et al. [2] reported 5-year progression-free survival (PFS) and overall survival (OS) rates of 40.7 % and 59.7 %, respectively. In this scenario, the identification of reliable predictors that could facilitate clinical decision-making is eagerly awaited.

Magnetic resonance imaging (MRI) is commonly used for treatment planning in head and neck squamous cell carcinoma (HNSCC) patients. Moreover, diffusion-weighted MR imaging (DWI) and dynamic contrast-enhanced MRI (DCE-MRI) are increasingly being used as functional imaging techniques for assessing tumour biology. While DWI is able to quantify the diffusion of water molecules in biological tissues, DCE-MRI is capable of assessing the tumour microvascular environment by determining the sequential changes in signal intensity over time. Currently, they can be incorporated into conventional MRI to examine HNSCC patients in a single examination session. ^{18}F-Fluorodeoxyglucose-positron emission tomography (^{18}F-FDG PET)/CT is another imaging technique widely used in the evaluation of HNSCC patients. It can provide valuable information about tissue metabolism as well as anatomical relationships. The clinical usefulness of DWI, DCE-MRI and ^{18}F-FDG PET/CT (most commonly alone and sporadically in combination) for predicting treatment outcome of HNSCC has been previously investigated, albeit with variable results [3–30]. The discrepancies may be related to the fact that most of the previous study series included heterogeneous groups of patients harbouring HNSCC of different mucosal sites with different treatments or different follow-up time periods. Different imaging scanners and non-standardized acquisition parameters are also contributory. In addition, some studies examined imaging measurements from primary tumours [3, 5–7, 10–12, 17–19, 26, 30], while others examined those from neck metastatic nodes [8, 9, 13–16, 23] or both [4, 20–22, 24, 25, 27–29]. Furthermore, only two series studies of combined use of DWI, DCE-MRI and ^{18}F-FDG PET/CT have been reported; notably, their results were limited to local control and neck control, respectively [5, 16]. The objective of the current study was to evaluate the predictive values of imaging parameters derived from these three imaging techniques (alongside clinical variables) for the 3 year-PFS and OS of OHSCC patients with nodal disease. To our knowledge, this is the first prospective study of using DWI, DCE-MRI and ^{18}F-FDG PET/CT to examine both primary tumours and neck metastatic nodes of OHSCC patients treated homogeneously with chemoradiation for survival prediction.

Materials and methods

Study participants and treatment approach

Patients with pathologically proven OHSCC scheduled for chemoradiation with curative intent were eligible for this prospective study. Ethics approval was granted by the institutional review board of our hospital (protocol no. 98-3582B) and the study complied with the tenets of the Declaration of Helsinki. Inclusion criteria for the study were as follows: (1) biopsy-proven diagnosis of OHSCC, (2) presence of regional

nodal metastasis, (3) ability to provide written informed consent and (4) no contraindications to MRI or ^{18}F-FDG PET/CT. Patients were excluded in the presence of a history of previous head or neck cancers, distant metastases or second malignancies.

All participants received intensity-modulated radiotherapy using 6-MV photon beams. The initial prophylactic field included gross tumour with at least 1-cm margins and neck lymphatics at risk for 46–56 Gy, then cone-down boost to the initial gross tumour area to 72 Gy. Concurrent chemotherapy consisted of intravenous cisplatin 50 mg/m^2 on day 1, oral tegafur 800 mg/day plus oral leucovorin 60 mg/day from day 1 to day 14. This regimen was delivered every 14 days [31]. Patients were monitored over a minimum follow-up of 12 months after treatment or until death.

Multimodal imaging

All patients underwent MRI and ^{18}F-FDG PET/CT before chemoradiation. MRI was performed on a 3-T scanner (Magnetom Trio with TIM, Siemens, Erlangen, Germany) as described previously [5, 16]. Briefly, conventional MRI of the head and neck region were performed in the axial and coronal projections with turbo spin echo. DWI was performed by using single shot spin-echo echo-planar imaging with a modified Stejskal–Tanner diffusion gradient pulsing scheme. Motion-probing gradients with a *b* value of 800 s/mm^2 were applied along three orthogonal directions. DCE-perfusion-weighted imaging (PWI) was performed by using a 3D T1-weighted spoiled gradient-echo sequence. A single dose of gadopentetate dimeglumine at a concentration of 0.1 mmol/kg body weight was injected at a rate of 3 mL/s into the antecubital vein, followed by a saline flush.

^{18}F-FDG PET/CT was performed using a Discovery ST 16 integrated PET/CT system (GE Healthcare, Milwaukee, WIUSA) as described previously [5, 16]. All patients fasted for at least 6 h before examination. Non-contrast-enhanced CT was performed from the head to the proximal thigh. About 1 h after injection of ^{18}F-FDG (370 MBq), emission scans were acquired with 3-min per table position.

Imaging parameters analysis

DWI-derived apparent diffusion coefficient (ADC) as well as DCE-MRI parameters, including the volume transfer rate constant (K^{trans}), relative extravascular extracellular space (V_e), relative vascular plasma volume (V_p) and the efflux rate constant (K_{ep}), from both primary tumours and the largest metastatic nodes were incorporated into analysis. Mean ADC values were measured on ADC maps by drawing the regions of interest (ROI) on the primary tumour and also the largest node respectively by the experienced head and neck radiologist, with the aid of the T2-weighted MR images and the T1-weighted post-contrast MR images to avoid cystic or necrotic areas. Because of their common use in clinical practice and high reproducibility [32], mean ADC values of the primary tumours (ADC-tumour) and nodes (ADC-node) were used in the current study. DCE-MRI was analysed with MATLAB 7.0 (The Mathworks, Natick, MA, USA). The signal intensities of the DCE-MRI data were converted from the contrast agent concentrations by solving their nonlinear relationship [33]. The extended Kety model [34] was used for the kinetic analysis in a voxel-wise manner. The arterial input function was extracted with the blind source separation algorithm [35]. ROIs were drawn on DCE-MR images by the same radiologist in a manner similar to that for the DWI analysis.

SUV and metabolic tumour volume (MTV) of primary tumours and regional nodal metastases were measured separately from attenuation-corrected ^{18}F-FDG PET images using the PMOD software (PMOD Technologies Ltd, Zurich, Switzerland). To minimize partial volume effects, we selected maximal SUV (SUV_{max}) for analysing the associations with survival endpoints. An SUV_{max} threshold of 2.5 was used to delineate MTV [19, 36]. Total lesion glycolysis (TLG) was calculated as the product of lesion mean SUV (SUV_{mean}) and MTV. The SUV_{max}, MTV and TLG and values of the primary tumour and cervical nodes were designated as SUV_{max}-tumour, SUV_{max}-node, MTV-tumour, MTV-node, and TLG-tumour, TLG-node, respectively.

Outcome determination and statistical analysis

PFS and OS were plotted using the Kaplan–Meier method. The optimal cutoff values for DCE-MRI-, DWI- and ^{18}F-FDG PET/CT-derived parameters were determined using the log-rank test based on the 3-year PFS rates observed in the entire cohort [17, 37]. Univariate Cox regression analysis was used to identify the predictors of PFS and OS rates. All of the prognostic variables in univariate analyses were entered into the multivariate Cox regression model, and stepwise forward selection was used to identify the independent predictors. Furthermore, prognostic models for PFS were provided separately for primary tumour and neck nodal parameters. All statistical analyses were performed using the SPSS software package (version 13.0; SPSS Inc., Chicago, IL, USA). The α error was set at 0.05 (two-tailed).

Results

Between August 2010 and July 2013, a total of 108 OHSCC patients were enrolled. Twenty-two patients were excluded from analysis: nine had primary tumours which were thin or excessively small in size, seven had cystic neck nodes and six

had significant artefacts on DWI or PWI images. Consequently, 86 OHSCC patients were available for analysis (6 female and 80 male; mean age 50 ± 9.54 years; tumour site: 45 oropharynx, 41 hypopharynx). All of our 86 patients had advanced stage disease: 4 (4.7 %) were stage III, 61 (70.9 %) in stage IVA and the remaining 21 (24.4 %) in stage IVB. The median follow-up time was 28 months in the entire study cohort (range 4–55 months) and 36 months for the censored cases (range 14–56 months). Of the 86 study patients, 33 patients (38.4 %) developed locoregional failure, 12 (18.6 %) distant metastasis and 4 (4.7 %) second primary tumours. At the time of analysis, 53 (62 %) patients were alive and 33 (38 %) were dead (29 died of disease and 4 died of other causes). The median PFS was 16 months (range 4–46 months). The 3-year PFS and OS rates were 54 % and 63 %, respectively. No significant association of survival rates with disease stage was evident (Fig. 1).

Tables 1 and 2 show the results of univariate and multivariate analyses for the prediction of survival in the entire study cohort. The following parameters were identified as significant predictors of PFS in univariate analyses: haemoglobin level < 14.3 g/dL ($P = 0.0027$), K^{trans}-tumour < 0.56 min^{-1} ($P = 0.0096$), K_{ep}-tumour < 3.79 min^{-1} ($P = 0.0474$), ADC-tumour > 0.86×10^{-3} mm^2/s ($P = 0.0162$), SUV_{max}-tumour > 19.44 ($P = 0.0098$), MTV-tumour > 42.62 cm^3 ($P = 0.0103$), TLG-tumour > 344.72 ($P = 0.0147$), K^{trans}-node < 0.86 min^{-1} ($P = 0.0419$), V_e-node < 0.23 ($P = 0.0117$), ADC-node > 1.14×10^{-3} mm^2/s ($P < 0.001$), MTV-node > 38.05 cm^3 ($P = 0.0306$) and TLG > 217.18 ($P = 0.0091$). Multivariate analysis of both primary tumour and nodal factors in combination identified K_{ep}-tumour ($P < 0.001$), TLG-tumour ($P = 0.049$), SUV_{max}-tumour ($P = 0.018$), V_e-node ($P = 0.004$) and ADC-node ($P < 0.001$) as independent predictors of PFS. When the prognostic models based on the primary tumour and neck nodes were analysed separately, slightly different risk factors were evident. The independent predictors identified in the primary tumour PFS model included age ($P = 0.002$), haemoglobin ($P = 0.035$), K_{ep}-tumour ($P = 0.02$), ADC-tumour ($P = 0.005$) and TLG-tumour ($P = 0.006$), while independent risk factors identified in the neck nodes PFS model included haemoglobin ($P = 0.008$), V_e-node ($P = 0.047$) and ADC-node ($P = 0.004$).

Univariate analysis identified age ($P = 0.0092$), haemoglobin level ($P = 0.0090$), K^{trans}-tumour ($P = 0.0026$), K^{trans}-node ($P = 0.0145$), V_e-node ($P = 0.0036$) and SUV_{max}-tumour ($P = 0.0402$) as significant predictors of OS. After allowance for potential confounders in multivariate stepwise Cox regression analysis, we found that K_{ep}-tumour < 3.79 cm^3 min^{-1} ($P = 0.002$), V_e-node < 0.23 ($P = 0.001$) and SUV_{max}-tumour >19.44 ($P = 0.004$) were independent predictors of OS.

We developed a three-point scoring system (0/1, 2, 3) based upon the sum of each of the three imaging parameters (i.e. K_{ep}-tumour, V_e-node and SUV_{max}-tumour) that were identified as independent predictors of both PFS and OS rates in multivariate analysis. The presence or absence of each risk factor (i.e. K_{ep}-tumour < 3.79 min^{-1}, V_e-node < 0.23 and SUV_{max}-tumour > 19.44) was assigned a score of 1 and 0, respectively, resulting in scores ranging from 0 to 3. We identified 4 patients with a score of 0, 40 patients with a score of 1, 37 patients with a score of 2, and 5 patients with a score of 3. Because of the low number of patients who scored 0, they were grouped together with those with a score of 1 for the purpose of analysis. The scoring system based upon the sum of each of the three imaging parameters significantly stratified both 3-year PFS (rates in the 0/1, 2, 3 groups: 72 %, 38 % and 0 %, respectively, $P < 0.0001$) and OS (rates in the 0/1, 2, 3 groups: 81 %, 46 % and 20 %, respectively, $P < 0.0001$) (Fig. 2). Four (80 %) of the five patients with a score of 3 died within 18 months of initial treatment. Of the 37 patients with a score of 2, 20 (54 %) died after a median period of 16 months. When patients with scores of 0/1 were considered as the reference category in multivariate Cox proportional hazard analysis, patients with a score of 2 were found to have significantly poorer PFS (HR = 3.1888, $P = 0.002$) and OS (HR = 3.868, $P = 0.001$). As expected, patients with a score of 3 showed the poorest PFS (HR = 12.682, $P < 0.001$) and OS (HR = 18.856, $P < 0.001$) rates (Table 3). Representative images of study patients with different scores are provided in Figs. 3 and 4.

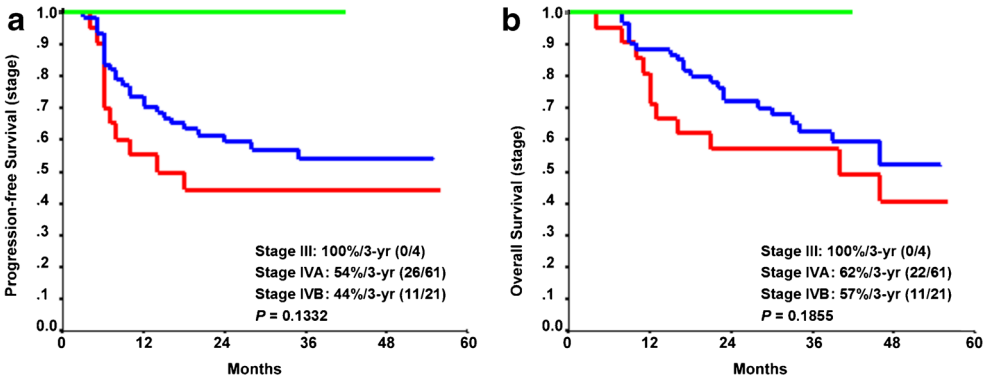

Fig. 1 Kaplan–Meier estimates of 3-year progression-free survival and overall survival rates in OHSCC patients ($n = 86$) stratified according tumour staging

Table 1 Univariate analyses of risk factors associated with 3-year progression-free survival and overall survival rates in OHSCC patients ($n = 86$)

Parameters (n, %)	Progression-FREE survival		Overall survival	
	% (n event)	P	% (n event)	P
Age (years)		0.0581		0.0092
< 65 (77, 89.5)	55 (32)		65 (27)	
≥ 65 (9, 10.5)	38 (5)		40 (6)	
Sex		0.3042		0.8704
Male (80, 93.0)	52 (36)		63 (31)	
Female (6, 7.0)	75 (1)		67 (2)	
Subsites		0.0947		0.9672
Oropharynx (45, 52.3)	61 (16)		60 (17)	
Hypopharynx (41, 47.7)	45 (21)		65 (16)	
Haemoglobin (g/dL)		0.0027		0.0090
> 14.30 (39, 45.3)	72 (10)		77 (9)	
≤ 14.30 (47, 54.7)	38 (27)		51 (24)	
T status		0.2341		0.5271
T1 (5, 5.8)	60 (2)		80 (2)	
T2 (20, 23.3)	55 (8)		76 (6)	
T3 (13, 15.1)	83 (2)		77 (3)	
T4a (40, 46.5)	41 (22)		50 (19)	
T4b (8, 9.3)	63 (3)		63 (3)	
N status		0.1443		0.2373
N1 (6, 7.0)	56 (2)		75 (1)	
N2b (48, 55.8)	57 (19)		67 (15)	
N2c (18, 20.9)	54 (8)		49 (9)	
N3 (14, 16.3)	38 (8)		57 (8)	
Stage		0.1503		0.1855
III (4, 4.7)	100 (0)		100 (0)	
IVA (61, 70.9)	54 (26)		62 (22)	
IVB (21, 24.4)	44 (11)		57 (11)	
K^{trans}-tumour (min^{-1})		0.0096		0.0026
> 0.56 (38, 44.2)	69 (11)		78 (9)	
≤ 0.56 (48, 55.8)	40 (26)		49 (24)	
V_p-tumour		0.2170		0.3212
> 0.008 (33, 38.4)	62 (12)		67 (11)	
≤ 0.008 (53, 61.6)	49 (25)		60 (22)	
V_e-tumour		0.2142		0.5103
> 0.22 (34, 39.5)	62 (12)		67 (12)	
≤ 0.22 (52, 60.5)	49 (25)		60 (21)	
K_{ep}-tumour (min^{-1})		0.0474		0.1116
> 3.79 (30, 34.9)	68 (9)		72 (9)	
≤ 3.79 (56, 65.1)	46 (28)		57 (24)	
ADC-tumour		0.0162		0.8161
< 0.86 (17, 19.8)	88 (2)		68 (6)	
≥ 0.86 (69, 80.2)	46 (35)		62 (27)	
SUV_{max}-tumour		0.0098		0.0402
< 19.44 (73, 84.9)	58 (28)		66 (25)	
≥ 19.44 (13, 15.1)	28 (9)		42(8)	
MTV-tumour (cm^3)		0.0103		0.1434
< 42.62 (74, 86.0)	59 (28)		67 (26)	
≥ 42.62 (12, 14.0)	22 (9)		38 (7)	
TLG-tumour		0.0147		0.0502
< 344.72 (75, 87.2)	58 (29)		68 (26)	
≥ 344.72 (11, 12.8)	24 (8)		30 (7)	
K^{trans}-node (min^{-1})		0.0419		0.0145
> 0.86 (12, 14.0)	83 (2)		92 (1)	
≤ 0.86 (74, 86.0)	47 (35)		57 (32)	
V_p-node		0.1942		0.0716
> 0.09 (9, 10.5)	78 (2)		89 (1)	
≤ 0.09 (77, 89.5)	50 (35)		60 (32)	
V_e-node		0.0117		0.0036
> 0.23 (26, 30.2)	74 (6)		87 (4)	
≤ 0.23 (60, 69.8)	45 (31)		52 (29)	
K_{ep}-node (min^{-1})		0.2221		0.6628
> 0.55 (76, 88.4)	55 (31)		63 (30	
≤ 0.55 (10, 11.6)	40 (6)		53 (3)	
ADC-node		0.0002		0.4939
< 1.14 (75, 87.2)	59 (28)		60 (30)	
≥ 1.14 (11, 12.8)	18 (9)		82 (3)	
SUV_{max}-node		0.0999		0.1151
< 16.35 (75, 87.2)	56 (30)		65 (26)	
≥ 16.35 (11, 12.8)	36 (7)		45 (7)	
MTV-node (cm^3)		0.0306		0.0936
< 38.05 (69, 80.2)	58 (26)		65 (23)	
≥ 38.05 (17, 19.8)	35 (11)		46 (10)	
TLG-node		0.0091		0.0564
< 217.18 (72, 83.7)	58 (27)		65 (24)	
≥ 217.18 (14, 16.3)	29 (10)		50 (9)	

OHSCC oropharyngeal or hypopharyngeal squamous cell carcinoma, K^{trans} volume transfer rate constant, K_{ep} efflux rate constant, V_p relative vascular plasma volume, V_e relative volume of extracellular extravascular space, *ADC* apparent diffusion coefficient, SUV_{max} maximum standardized uptake value, *MTV* metabolic tumour volume, *TLG* total lesion glycolysis

Discussion

This prospective study showed that K_{ep}-tumour, V_e-node and SUV_{max}-tumour were independent predictors of both PFS and OS rates of OHSCC patients with nodal metastasis treated with chemoradiation. Integration of these imaging factors into a prognostic scoring system results in an accurate classification of patients outcomes. Differences in primary tumour- and node-related imaging prognosticators reflect different intrinsic biologic characteristics of either sites, suggesting that their

Table 2 Multivariate analyses of risks factors associated with 3-year progression-free survival and overall survival in OHSCC patients ($n = 86$)

Characteristics	Progression-free survival		Overall survival	
	P	HR, 95 % CI	*P*	HR, 95 %CI
Age(years)	NS		NS	
< 65 (77, 89.5)				
≥ 65 (9, 10.5)				
Haemoglobin(g/dl)	NS		NS	
> 14.30 (39, 45.3)				
≤ 14.30 (47, 54.7)				
K^{trans}-tumour (min^{-1})	NS		NS	
> 0.56 (38, 44.2)				
≤ 0.56 (48, 55.8)				
K_{ep}-tumour (min^{-1})	0.001		0.002	
> 3.79		Reference		Reference
≤ 3.79		3.891 (1.728–8.762)		3.655 (1.600–8.352)
ADC-tumour	NS		NS	
< 0.86 (17, 19.8)				
≥ 0.86 (69, 80.2)				
SUV_{max}-tumour	0.025		0.004	
< 19.44		Reference		Reference
≥ 19.44		2.532 (1.121–5.715)		3.477 (1.505–8.031)
MTV-tumour (cm^3)	NS		NS	
< 42.62 (74, 86.0)				
≥ 42.62 (12, 14.0)				
TLG-tumour	0.038		NS	
< 344.72		Reference		
≥ 344.72		2.449 (1.051–5.705)		
K^{trans}-node (min^{-1})	NS		NS	
> 0.86 (12, 14.0)				
≤ 0.86 (74, 86.0)				
V_e-node	0.004		0.001	
> 0.23		Reference		Reference
≤ 0.23		4.092 (1.583–10.578)		5.929 (1.987–17.690)
ADC-node	<0.001		NS	
< 1.14 (75, 87.2)		Reference		
≥ 1.14 (11, 12.8)		4.858 (2.089–11.300)		
MTV-node (cm^3)	NS		NS	
< 38.05 (69, 80.2)				
≥ 38.05 (17, 19.8)				
TLG-node	NS		NS	
< 217.18 (72, 83.7)				
≥ 217.18 (14, 16.3)				

OHSCC oropharyngeal or hypopharyngeal squamous cell carcinoma, *HR* hazard ratio, *CI* confidence interval, *NS* not significant, K^{trans} volume transfer rate constant, K_{ep} efflux rate constant, V_e relative volume of extracellular extravascular space, *ADC* apparent diffusion coefficient, SUV_{max} maximum standardized uptake value, *MTV* metabolic tumour volume, *TLG* total lesion glycolysis

functional parameters should be measured separately and evaluated together.

DCE-MRI can provide the pharmacokinetic parameters of the selected regions and has been used to predict treatment outcomes of HNSCC patients. Nodal K^{trans} has been reported to be higher in patients who achieved complete response after treatment as compared with partial responders [9]. Higher pretreatment nodal K^{trans} values have been associated with

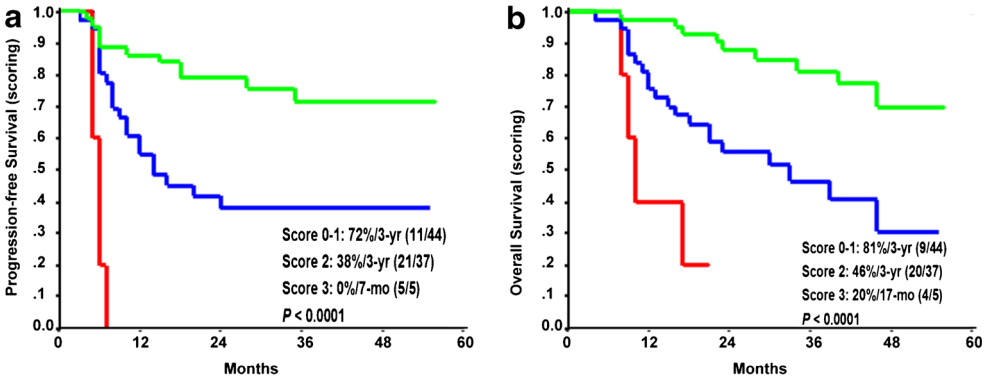

Fig. 2 Kaplan–Meier estimates of progression-free survival and overall survival in OHSCC patients ($n = 86$) stratified according to the three-point scoring system (0/1, 2, 3) based upon the sum of each of the three imaging parameters (K_{ep}-tumour, V_e-node and SUV_{max}-tumour)

disease-free survival rates [14], whereas both nodal K^{trans} and nodal V_e have been found to be significant predictors of PFS and OS [15]. Notably, Jansen et al. [13] reported that nodal K^{trans} and SUV_{mean} may improve the prediction of short-term response to therapy as compared with either parameter alone. Similarly, another study has shown that the combined assessment of DWI- and DCE-MRI-derived parameters from both primary tumours and nodal masses significantly predicted response to chemoradiation, whereas each parameter alone did not [4]. We have previously shown that tumour K^{trans} was a clinically useful predictor of local control after chemoradiation in OHSCC patients [5]. In another report from our group [16], nodal V_e and nodal ADC (but not K^{trans}) were identified as independent prognostic factors for neck control. Taken together, these results suggest that the pretreatment K^{trans} may show promise for predicting treatment outcome to chemoradiation therapy in HNSCC, but its significance can vary among different tumour types, selected ROI locations and study endpoints. In the present study, pretreatment K_{ep}-tumour and V_e-node—but not K^{trans}-tumour or K^{trans}-node—were identified as independent predictors of both PFS and OS in OHSCC patients treated with chemoradiation.

K_{ep} is the efflux rate constant describing the contrast transfer between the extravascular extracellular space and plasma and, hence, related to tissue vascular permeability and surface area [38, 39]. K_{ep} can predict response to radiation in patients with cervix cancer [40] and its values are significantly reduced in the hypoxic nodes of patients with HNSCC [41]. Higher K_{ep} values have been also associated with better treatment response in patients with liver metastases from colorectal cancer [42]. The higher K_{ep}-value may reflect a greater exchange of therapeutic agents between plasma and the extracellular extravascular space, ultimately favouring drug delivery and resulting in better treatment outcomes. Consistently, high K_{ep}-tumour values were significantly associated with better PFS and OS rates in the current study.

V_e is another DCE-MRI-derived parameter that reflects the extravascular extracellular space. Previous studies identified V_e as an independent predictor of OS in patients with colorectal cancer [43], as well as of both PFS and OS in HNSCC [15]. Notably, we previously identified V_e as one of the independent predictors of neck control in OHSCC patients [16]. However, some other previous HNSCC studies [4, 9, 13] reported negative results on the value of V_e for predicting treatment response. Our current observation that V_e-node predicted survival rates in OHSCC patients suggests that the nodal extravascular extracellular space could have prognostic significance in determining prognosis in this patient group.

The potential role of DWI-derived ADC for predicting radiotherapy or chemoradiation outcomes in HNSCC is still a matter of debate [3–8, 10–12, 16]. Some DWI studies have shown that tumours with pretreatment high ADC values are associated with local failure [3, 7], neck failure [8, 16] and survival outcomes [10–12], but other reports failed to identify such an association [4–6]. In this study, we were unable to demonstrate a significant association of ADC values with both PFS and OS rates in multivariate analysis, suggesting that DCE-MRI is superior to DWI for predicting prognosis in OHSCC patients treated with chemoradiation. Recently, intravoxel incoherent motion (IVIM) imaging was developed as a novel DWI technique that allows a separate quantification of diffusion and perfusion effects. Previous studies have

Table 3 Multivariate analyses of 3-year progression-free survival and overall survival according to the prognostic scoring system based on multimodal imaging (including K_{ep}-tumour, SUV_{max}-tumour and V_e-node

	Progression-free survival *P*, HR, 95 % CI	Overall survival *P*, HR, 95 % CI
Score 0–1 ($n = 44$)	Reference	Reference
Score 2 ($n = 37$)	0.002, 3.188 (1.526–6.661)	0.001, 3.868 (1.750–8.549)
Score 3 ($n = 5$)	<0.001, 12.682 (3.575–44.984)	<0.001, 18.856 (4.117–86.364)

K_{ep} efflux rate constant, *SUV max* maximum standardized uptake value, V_e relative volume of extracellular extravascular space, *HR* hazard ratio, *CI* confidence interval

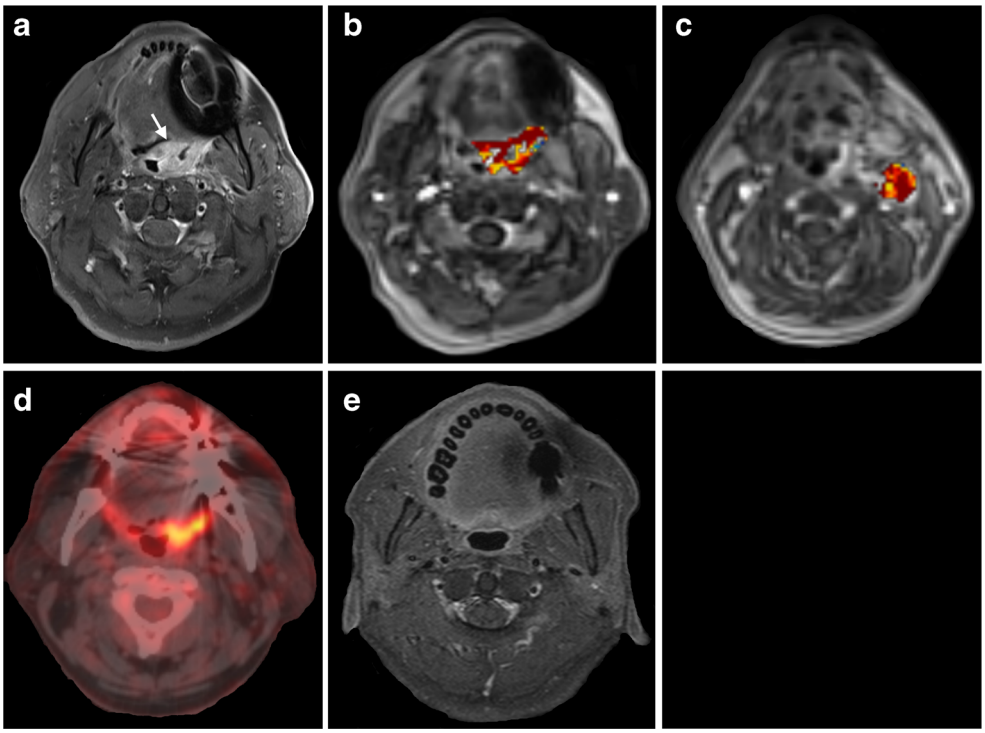

Fig. 3 A 45-year-old male patient with oropharyngeal SCC and a score of 0. **a** Pretreatment axial-enhanced MRI image shows a left oropharyngeal tumour (*arrow*). **b** The corresponding DCE-MRI image with an overlaid K_{ep} map of the primary tumour shows a K_{ep}-tumour value of 5.16 min^{-1}. **c** The corresponding DCE-MRI image with an overlaid V_e map of the node shows a V_e-node value of 0.51. **d** The corresponding ^{18}F-FDG PET/CT image showed an SUV_{max}-tumour value of 8.38. **e** Post-treatment axial-enhanced MRI shows complete regression of the primary tumour. After 42 months of follow-up, the patients remained disease-free

shown the utility of IVIM for characterizing head and neck tumours [44, 45], but its role in predicting survival deserves further scrutiny.

There is a plethora of published articles about the prognosis prediction of ^{18}F-FDG PET for HNSCC, but the prognostic significance of its parameters remains controversial. Among the imaging parameters of ^{18}F-FDG PET/CT, SUV_{max} is the most common semiquantitative measure used for expressing tumour FDG uptake. Compared with SUV_{mean}, SUV_{max} is less influenced by the partial volume effect and is not affected by the method used to analyse the lesion boundaries [17–19, 21, 46]. High SUV_{max} is recognized as a significant predictor

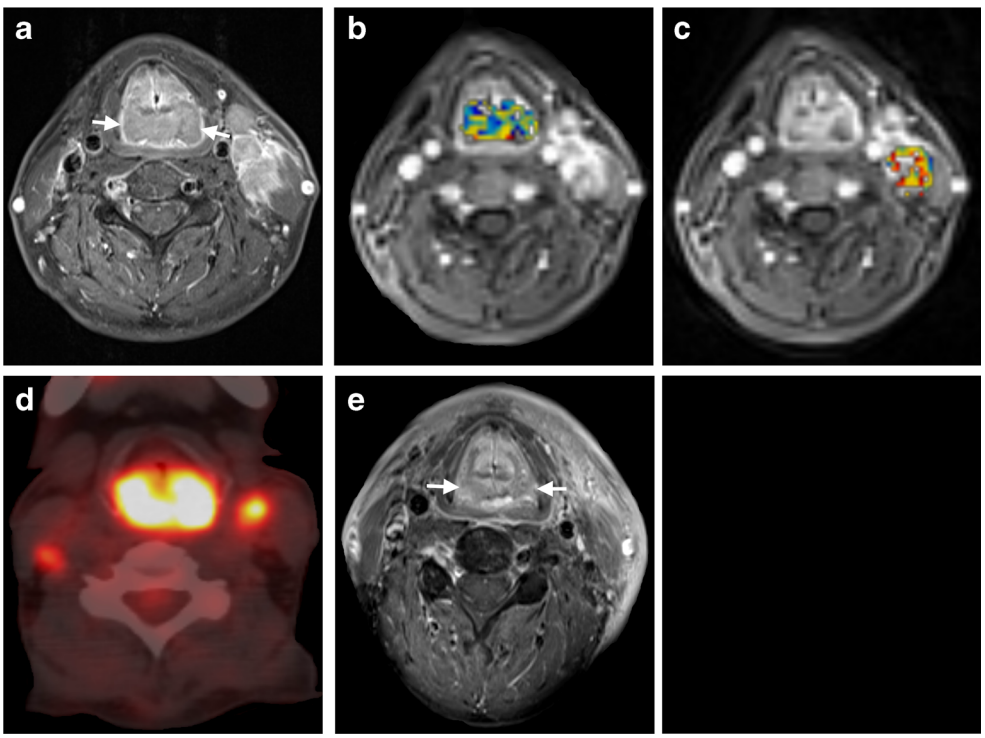

Fig. 4 A 46-year-old male patient with hypopharyngeal SCC and a score of 3. **a** Pretreatment axial-enhanced MRI image shows a posterior wall hypopharyngeal tumour (*arrows*). **b** The corresponding DCE-MRI image with an overlaid K_{ep} map of the primary tumour shows a K_{ep}-tumour value of 1.62 min^{-1}. **c** The corresponding DCE-MRI image with an overlaid V_e map of the node shows a V_e-node value of 0.21. **d** The corresponding ^{18}F-FDG PET/CT image shows an SUV_{max}-tumour value of 21.52. **e** Post-treatment axial-enhanced MRI shows a residual primary tumour (*arrows*), which was subsequently confirmed by pharyngolaryngectomy. The patient died at 17 months after chemoradiation

of poor survival [17, 18, 21–24, 26, 30]. Interestingly, Schwartz et al. [22] found that SUV_{max} of the primary tumour—but not that of metastatic nodes—can predict survival, whereas another study reported the opposite [21]. Furthermore, other investigators identified an association of survival with MTV or TLG but not with SUV [19, 20, 25, 27–29]. In this study with OHSCC homogeneously treated with chemoradiation, SUV_{max}-tumour was the only ^{18}F-FDG PET-derived parameter independently associated with both survival endpoints, possibly as a proxy of an increased tumour biological aggressiveness [17, 26].

Notably, the TNM stage (at present the most commonly used prognostic system) did not correlate significantly with either PFS or OS (Fig. 1) as our proposed scoring system did (Fig. 2). Pending external validation, we believe that our multimodal imaging approach could improve the prognostic stratification of OHSCC patients scheduled for chemoradiation. In clinical practice, our scoring system may be helpful for identifying a subgroup of OPSCC patients at high risk of poor survival after chemoradiation. These subjects may be considered as potential suitable candidates for surgery or trials of novel treatment approaches, including molecular targeted therapy. On the other hand, integrated PET/MRI is a novel imaging technology that has been recently introduced into clinical practice. Because of its capability to obtain both PET and MRI data in a single examination, hybrid PET/MRI may not only help to compensate the interpretation pitfalls of FDG uptake [47] but can also provide simultaneous functional and metabolic information that would be more accurate than the data that might be obtained by separately performing PET/CT and MRI at different time intervals. Future studies are needed to investigate whether PET/MRI can outperform DWI MRI, DCE-MRI, PET/CT or the combination of these techniques.

Our study has limitations that need to be mentioned. First, the single-centre nature of the study requires independent replication of the results by different research groups. Despite its use in previous studies [2, 31], our chemotherapy scheme remains uncommon. Consequently, translation of our results to other centres would be hampered. Second, we acknowledge that both DWI- and DCE-MRI-derived parameters are dependent of the choice of the ROI. However, a single experienced head and neck radiologist drew all ROIs in the current study. Third, DCE-MRI and DWI analyses were performed on slices where the primary lesion and the affected node were at their greatest diameter, because we lacked a software package able to perform reproducible analysis of the entire primary tumour volume and all regional nodal metastases. Fourth, our model might not be applicable to all patients, particularly those with small-sized, cystic lesions or distortion artefacts. Finally, because the human papillomavirus (HPV) status was not routinely assessed in our institution during the study period, complete data on HPV infection were not available. HPV infections may have a different impact on outcomes to chemoradiation in hypopharyngeal versus oropharyngeal SCC. However, PFS and OS rates did not differ significantly in our patients with hypopharyngeal versus oropharyngeal SCC, making the confounding effect of HPV infections likely to be non-influential in this study.

Conclusions

Our results suggest that K_{ep}-tumour, V_e-node and SUV_{max}-tumour are independent prognostic factors for OHSCC patients treated with chemoradiation. We demonstrate that the application of a scoring system based on multimodal imaging can permit reliable prognosis prediction in OHSCC patients scheduled for chemoradiation, ultimately improving treatment planning.

Acknowledgments The scientific guarantor of this publication is Shu-Hang Ng. The authors of this manuscript declare no relationships with any companies whose products or services may be related to the subject matter of the article. This study has received funding by two grants (99-2314-B-182A-095-MY3 and NSC 102-2314-B-182A-098 -MY2) from the National Science Council-Taiwan. The imaging facility was supported by the Imaging Core Laboratory of Institute for Radiological Research and Center for Advanced Molecular Imaging and Translation. The authors would like to thank the Neuroscience Research Center, Chang Gung Memorial Hospital, Imaging Core Laboratory of Institute for Radiological Research, Chang Gung University / Chang Gung Memorial Hospital, Linkou and the Healthy Aging Center, Chang Gung University for providing support. Two of the authors has significant statistical expertise (Chun-Ta Liao and Lan-Yan Yang). Institutional review board approval was obtained. The Institutional Review Board of the Chang Gung Memorial Hospital approved the study protocol (protocol no. 98-3582B) in December 2009. Written informed consent was obtained from all patients in this study. Some study subjects or cohorts have been previously reported with different research goals in the following two published papers:

Ng SH, Lin CY, Chan SC bet al. (2013) Dynamic contrast-enhanced MR imaging predicts local control in oropharyngeal or hypopharyngeal squamous cell carcinoma treated with chemoradiotherapy. PLoS One 8:e72230

Ng SH, Lin CY, Chan SC et al (2014) Clinical utility of multimodality imaging with dynamic contrast-enhanced MRI, diffusion-weighted MRI, and 18F-FDG PET/CT for the prediction of neck control in oropharyngeal or hypopharyngeal squamous cell carcinoma treated with chemoradiation. PLoS One 9:e115933

Methodology: prospective, diagnostic or prognostic study, performed at one institution.

References

1. Urba SG, Moon J, Giri PG et al (2005) Organ preservation for advanced resectable cancer of the base of tongue and hypopharynx: a Southwest Oncology Group Trial. J Clin Oncol 23:88–95
2. Wang HM, Hsu CL, Hsieh CH et al (2014) Concurrent chemoradiotherapy using cisplatin, tegafur, and leucovorin for advanced squamous cell carcinoma of the hypopharynx and oropharynx. Biomed J 37:133–140
3. Ohnishi K, Shioyama Y, Hatakenaka M et al (2011) Prediction of local failures with a combination of pretreatment tumor volume and apparent diffusion coefficient in patients treated with definitive radiotherapy for hypopharyngeal or oropharyngeal squamous cell carcinoma. J Radiat Res 52:522–530
4. Chawla S, Kim S, Dougherty L et al (2013) Pretreatment diffusion-weighted and dynamic contrast-enhanced MRI for prediction of

local treatment response in squamous cell carcinomas of the head and neck. AJR Am J Roentgenol 200:35–43
5. Ng SH, Lin CY, Chan SC et al (2013) Dynamic contrast-enhanced MR imaging predicts local control in oropharyngeal or hypopharyngeal squamous cell carcinoma treated with chemoradiotherapy. PLoS One 8, e72230
6. King AD, Mo FK, Yu KH et al (2010) Squamous cell carcinoma of the head and neck: diffusion-weighted MR imaging for prediction and monitoring of treatment response. Eur Radiol 20:2213–2220
7. Hatakenaka M, Nakamura K, Yabuuchi H et al (2011) Pretreatment apparent diffusion coefficient of the primary lesion correlates with local failure in head-and-neck cancer treated with chemoradiotherapy or radiotherapy. Int J Radiat Oncol Biol Phys 81:339–345
8. Kim S, Loevner L, Quon H et al (2009) Diffusion-weighted magnetic resonance imaging for predicting and detecting early response to chemoradiation therapy of squamous cell carcinomas of the head and neck. Clin Cancer Res 15:986–994
9. Kim S, Loevner LA, Quon H et al (2010) Prediction of response to chemoradiation therapy in squamous cell carcinomas of the head and neck using dynamic contrast-enhanced MR imaging. AJNR Am J Neuroradiol 31:262–268
10. Nakajo M, Nakajo M, Kajiya Y et al (2012) FDG PET/CT and diffusion-weighted imaging of head and neck squamous cell carcinoma: comparison of prognostic significance between primary tumor standardized uptake value and apparent diffusion coefficient. Clin Nucl Med 37:475–480
11. Hatakenaka M, Nakamura K, Yabuuchi H et al (2014) Apparent diffusion coefficient is a prognostic factor of head and neck squamous cell carcinoma treated with radiotherapy. Jpn J Radiol 32:80–89
12. Lambrecht M, Van Calster B, Vandecaveye V et al (2014) Integrating pretreatment diffusion weighted MRI into a multivariable prognostic model for head and neck squamous cell carcinoma. Radiother Oncol 110:429–434
13. Jansen JF, Schoder H, Lee NY et al (2012) Tumor metabolism and perfusion in head and neck squamous cell carcinoma: pretreatment multimodality imaging with 1H magnetic resonance spectroscopy, dynamic contrast-enhanced MRI, and [18F]FDG-PET. Int J Radiat Oncol Biol Phys 82:299–307
14. Chawla S, Kim S, Loevner LA et al (2011) Prediction of disease-free survival in patients with squamous cell carcinomas of the head and neck using dynamic contrast-enhanced MR imaging. AJNR Am J Neuroradiol 32:778–784
15. Shukla-Dave A, Lee NY, Jansen JF et al (2012) Dynamic contrast-enhanced magnetic resonance imaging as a predictor of outcome in head-and-neck squamous cell carcinoma patients with nodal metastases. Int J Radiat Oncol Biol Phys 82:1837–1844
16. Ng SH, Lin CY, Chan SC et al (2014) Clinical utility of multimodality imaging with dynamic contrast-enhanced MRI, diffusion-weighted MRI, and 18F-FDG PET/CT for the prediction of neck control in oropharyngeal or hypopharyngeal squamous cell carcinoma treated with chemoradiation. PLoS One 9, e115933
17. Allal AS, Slosman DO, Kebdani T, Allaoua M, Lehmann W, Dulguerov P (2004) Prediction of outcome in head-and-neck cancer patients using the standardized uptake value of 2-[18F]fluoro-2-deoxy-D-glucose. Int J Radiat Oncol Biol Phys 59:1295–1300
18. Torizuka T, Tanizaki Y, Kanno T et al (2009) Prognostic value of 18F-FDG PET in patients with head and neck squamous cell cancer. AJR Am J Roentgenol 192:W156–W160
19. Seol YM, Kwon BR, Song MK et al (2010) Measurement of tumor volume by PET to evaluate prognosis in patients with head and neck cancer treated by chemo-radiation therapy. Acta Oncol 49:201–208
20. Vernon MR, Maheshwari M, Schultz CJ et al (2008) Clinical outcomes of patients receiving integrated PET/CT-guided radiotherapy for head and neck carcinoma. Int J Radiat Oncol Biol Phys 70:678–684
21. Demirci U, Coskun U, Akdemir UO et al (2011) The nodal standard uptake value (SUV) as a prognostic factor in head and neck squamous cell cancer. Asian Pac J Cancer Prev 12:1817–1820
22. Schwartz DL, Rajendran J, Yueh B et al (2004) FDG-PET prediction of head and neck squamous cell cancer outcomes. Arch Otolaryngol Head Neck Surg 130:1361–1367
23. Liao CT, Chang JT, Wang HM et al (2009) Preoperative [18F]-fluorodeoxyglucose positron emission tomography standardized uptake value of neck lymph nodes may aid in selecting patients with oral cavity squamous cell carcinoma for salvage therapy after relapse. Eur J Nucl Med Mol Imaging 36:1783–1793
24. Kubicek GJ, Champ C, Fogh S et al (2010) FDG-PET staging and importance of lymph node SUV in head and neck cancer. Head Neck Oncol 2:19
25. Tang C, Murphy JD, Khong B et al (2012) Validation that metabolic tumor volume predicts outcome in head-and-neck cancer. Int J Radiat Oncol Biol Phys 83:1514–1520
26. Kim SY, Roh JL, Kim MR et al (2007) Use of 18F-FDG PET for primary treatment strategy in patients with squamous cell carcinoma of the oropharynx. J Nucl Med 48:752–757
27. Lim R, Eaton A, Lee NY et al (2012) 18F-FDG PET/CT metabolic tumor volume and total lesion glycolysis predict outcome in oropharyngeal squamous cell carcinoma. J Nucl Med 53:1506–1513
28. Chung MK, Jeong HS, Park SG et al (2009) Metabolic tumor volume of [18F]-fluorodeoxyglucose positron emission tomography/computed tomography predicts short-term outcome to radiotherapy with or without chemotherapy in pharyngeal cancer. Clin Cancer Res 15:5861–5868
29. Cheng NM, Chang JT, Huang CG et al (2012) Prognostic value of pretreatment (18)F-FDG PET/CT and human papillomavirus type 16 testing in locally advanced oropharyngeal squamous cell carcinoma. Eur J Nucl Med Mol Imaging. doi:10.1007/s00259-012-2186-9
30. Liao CT, Chang JT, Wang HM et al (2009) Pretreatment primary tumor SUVmax measured by FDG-PET and pathologic tumor depth predict for poor outcomes in patients with oral cavity squamous cell carcinoma and pathologically positive lymph nodes. Int J Radiat Oncol Biol Phys 73:764–771
31. Wang HM, Wang CS, Chen JS, Chen IH, Liao CT, Chang TC (2002) Cisplatin, tegafur, and leucovorin: a moderately effective and minimally toxic outpatient neoadjuvant chemotherapy for locally advanced squamous cell carcinoma of the head and neck. Cancer 94:2989–2995
32. Noij DP, Pouwels PJ, Ljumanovic R et al (2015) Predictive value of diffusion-weighted imaging without and with including contrast-enhanced magnetic resonance imaging in image analysis of head and neck squamous cell carcinoma. Eur J Radiol 84:108–116
33. Schabel MC, Parker DL (2008) Uncertainty and bias in contrast concentration measurements using spoiled gradient echo pulse sequences. Phys Med Biol 53:2345–2373
34. Tofts PS, Brix G, Buckley DL et al (1999) Estimating kinetic parameters from dynamic contrast-enhanced T(1)-weighted MRI of a diffusable tracer: standardized quantities and symbols. J Magn Reson Imaging 10:223–232
35. Lin YC, Chan TH, Chi CY et al (2012) Blind estimation of the arterial input function in dynamic contrast-enhanced MRI using purity maximization. Magn Reson Med. doi:10.1002/mrm.24144
36. Chan SC, Hsu CL, Yen TC, Ng SH, Liao CT, Wang HM (2013) The role of 18F-FDG PET/CT metabolic tumour volume in predicting survival in patients with metastatic nasopharyngeal carcinoma. Oral Oncol 49:71–78
37. Halfpenny W, Hain SF, Biassoni L, Maisey MN, Sherman JA, McGurk M (2002) FDG-PET. A possible prognostic factor in head and neck cancer. Br J Cancer 86:512–516

38. Tofts PS, Kermode AG (1991) Measurement of the blood-brain barrier permeability and leakage space using dynamic MR imaging. 1. Fundamental concepts. Magn Reson Med 17:357–367
39. Tofts PS (1997) Modeling tracer kinetics in dynamic Gd-DTPA MR imaging. J Magn Reson Imaging 7:91–101
40. Zahra MA, Tan LT, Priest AN et al (2009) Semiquantitative and quantitative dynamic contrast-enhanced magnetic resonance imaging measurements predict radiation response in cervix cancer. Int J Radiat Oncol Biol Phys 74:766–773
41. Jansen JF, Schoder H, Lee NY et al (2010) Noninvasive assessment of tumor microenvironment using dynamic contrast-enhanced magnetic resonance imaging and 18F-fluoromisonidazole positron emission tomography imaging in neck nodal metastases. Int J Radiat Oncol Biol Phys 77:1403–1410
42. Coenegrachts K, Bols A, Haspeslagh M, Rigauts H (2012) Prediction and monitoring of treatment effect using T1-weighted dynamic contrast-enhanced magnetic resonance imaging in colorectal liver metastases: potential of whole tumour ROI and selective ROI analysis. Eur J Radiol 81: 3870–3876
43. Koh TS, Ng QS, Thng CH, Kwek JW, Kozarski R, Goh V (2013) Primary colorectal cancer: use of kinetic modeling of dynamic contrast-enhanced CT data to predict clinical outcome. Radiology 267:145–154
44. Sumi M, Nakamura T (2014) Head and neck tumours: combined MRI assessment based on IVIM and TIC analyses for the differentiation of tumors of different histological types. Eur Radiol 24:223–231
45. Zhang SX, Jia QJ, Zhang ZP et al (2014) Intravoxel incoherent motion MRI: emerging applications for nasopharyngeal carcinoma at the primary site. Eur Radiol 24:1998–2004
46. Higgins KA, Hoang JK, Roach MC et al (2012) Analysis of pretreatment FDG-PET SUV parameters in head-and-neck cancer: tumor SUVmean has superior prognostic value. Int J Radiat Oncol Biol Phys 82:548–553
47. Purohit BS, Ailianou A, Dulguerov N, Becker CD, Ratib O, Becker M (2014) FDG-PET/CT pitfalls in oncological head and neck imaging. Insights Imaging 5:585–602